Transplantation of exogenous mitochondria mitigates myocardial dysfunction after cardiac arrest

Zhen Wang [1]†, Jie Zhu [1]†, Mengda Xu [2], Xuyuan Ma [3], Maozheng Shen [3], Jingyu Yan,[2] Guosheng Gan[1, 2, *], Xiang Zhou [1, 2, *]

1. The First School of Clinical Medicine, Southern Medical University, Guangzhou, China
2. Department of Anesthesiology, General hospital of central theater command of PLA, Wuhan, China
3. Base of Central Theater Command of People's Liberation Army, Hubei University of Medicine, Wuhan, China

*Corresponding author to Guosheng Gan(526193186@qq.com), and Xiang Zhou(zhouxiang188483@126.com)

†These authors contributed equally to this work and should be considered as co-first authors

Abstract The incidence of post-cardiac arrest myocardial dysfunction (PAMD) is high, and there is currently no effective treatment available. This study aims to investigate the protective effects of exogenous mitochondrial transplantation. Exogenous mitochondrial transplantation can enhance myocardial function and improve the survival rate. Mechanistic studies suggest that mitochondrial transplantation can limit impairment in mitochondrial morphology, augment the activity of mitochondrial complexes II and IV, and raise ATP level. As well, mitochondrial therapy ameliorated oxidative stress imbalance, reduced myocardial injury, and thus improved PAMD after cardiopulmonary resuscitation (CPR).

Keywords: mitochondrial transplantation; cardiac arrest; post-cardiopulmonary resuscitation myocardial dysfunction; cardioprotection; ischemia

Introduction

Cardiac arrest (CA) is a life-threatening event and that is followed by post-cardiac arrest myocardial dysfunction (PAMD) after the return of spontaneous circulation (ROSC). PAMD exhibits degrees of systolic and diastolic dysfunction. The heart requires up to 30 kg of ATP daily to maintain systolic function (***Hall, et al.**,**2014***). Due to the high energy requirements of the myocardium, mitochondria make up approximately one-third of the volume of cardiomyocytes (***Cao, et al.**,**2023***). The occurrence of PAMD is associated with mitochondrial damage with increased mitochondrial volume, accumulation of calcium ions, a diminution in complex activity, and a decrease in phosphate synthesis (***Huang, et al.**,**2015***; ***McCully, et al.**,**2023***; ***Su, et al.**,**2021***; ***Tsai, et al.**,**2021***). Myocardium, as a high energy-consuming tissue, is very susceptible to energy depletion due to mitochondrial dysfunction. After mitochondrial injury, cytoplasmic and mitochondrial calcium overload prevents full relaxation of cardiomyocytes and can release cytochrome C to activate mitochondrial apoptotic pathways. This process contributes to the development of PAMD (***Gazmuri and Radhakrishnan**,**2012***; ***Su, et al.**,**2021***). Therefore, maintaining cardiomyocyte mitochondrial function after cardiopulmonary resuscitation (CPR) could be useful for cell survival and tissue homeostasis.

Transplantation of mitochondria isolated from non-ischemic or allogeneic tissues promoted myocardial recovery after regional ischemia (***McCully, et al.**,**2009***). Although the safety and efficacy of this approach have been verified (***Ali, et al.**,**2021***;

Jia, et al.*,*2022), effectiveness of mitochondrial transplantation in treating myocardial injury following CA remains to be demonstrated. Herein, we performed mitochondrial transplantation in rats following CPR to observe its effects on cardiac function and prognosis and explored its potential mechanism of action.

Results

CA-CPR model

No significant differences in weight or temperature were found between any groups before modeling. There was no significant difference in CA induction or CPR duration among the normal saline (NS), respiration buffer (Vehicle), and mitochondrial suspension (Mito) groups. Compared with the Sham group, the other three groups tended to receive less anesthetic (Table 1).

Mitochondrial transplantation improves cardiac function and does not alter hemodynamics in rats.

Echocardiography revealed no differences in cardiac function among the groups prior to CA-CPR. Compared with the baseline, the left ventricular ejection fraction of rats subjected to CA-CPR significantly decreased at 1 hour after ROSC, and gradually improved over time ($P<0.05$; Fig. 2A, 2B). Of note, the level of cardiac-function impairment in the Mito group was significantly reduced 4 hours after ROSC compared with the NS and Vehicle groups ($P<0.05$).

There was no statistically significant difference between MAP and HR at any observational timepoints ($P>0.05$, Fig. 2C). In the NS, Vehicle and Mito groups, the mean arterial pressure (MAP) and heart rate (HR) decreased at 1, 2, 3, and 4 hours after ROSC, reaching their nadir at 1 hour. Subsequently, MAP and HR increased gradually but did not show any statistically significant differences compared with the Sham group.

Mitochondrial transplantation improves the 72-hour survival rate after CPR in rats.

In animals not treated with mitochondria, Kaplan-Meier analysis found a rapid drop in the survival rate of rats within 24 hours after ROSC. In contrast, the survival rate of the Mito group was significantly higher than that of the NS and Vehicle groups ($P<0.05$, Fig. 2D).

Viability and of isolated mitochondria.

To evaluate the mitochondrial membrane potential ($\Delta\Psi$m), JC-1 dye was used JC-1 dye aggregates in healthy mitochondria and fluoresces red. Upon the decrease of $\Delta\Psi$ m, JC-1 can only exists as monomers and fluoresces green. A more pronounced red fluorescence indicates a higher number of normal mitochondria. This finding suggests that the majority of mitochondria extracted from the gastrocnemius muscle can maintain normal mitochondrial function (Fig. 3A). Mitochondria purity was confirmed by immunoblotting for TOM20 (a mitochondrial-specific protein) and COX □ in both skeletal samples and isolated mitochondrial proteins. GAPDH was only detected in skeletal muscle proteins (Fig. 3B).

Effects of mitochondrial transplantation on cardiomyocyte mitochondria.

Transplanted Mitochondria are internalized by cardiomyocytes. To verify the transfer of mitochondria to cardiomyocytes, we labeled the mitochondria with Mito-Tracker Red and transplanted them into the myocardium via the femoral vein. We primarily seek evidence of mitochondrial internalization within the endocardium, as initial injury occurs in this region during myocardial ischemia (***Kuwada and Takenaka***,***2000***). Four hours after injection, analysis of tissue sections found labelled mitochondria in endocardium (Fig. 4). The uptake of exogenous mitochondria was also observed in the myocardium and epicardium (supplement Fig. 1).

Mitochondrial transplantation does not alter the mass of myocardial mitochondria. The TOM20 protein is constitutively expressed in the outer membrane of mitochondria, and its abundance correlates with the amount of mitochondrial mass (***Abrigo, et al.****,****2023***). To investigate the potential increase of mitochondrial mass in myocardial tissue through mitochondrial transplantation, the expression of TOM20 was assessed in each group using tissue immunofluorescence staining. After 4 hours of ROSC, there was no significant difference in TOM20 level (as reflected by fluorescence intensity) among all groups, suggesting that mitochondrial transplantation did not increase the mass of mitochondria in heart. (Fig. 5A, 5B).

Mitochondrial transplantation improves cardiac mitochondrial structure.

Transmission electron microscopy (TEM) micrographs of heart tissues were presented in Fig. 5C. By using the Flameng method, the extent of mitochondrial damage in heart tissues across the four groups was assessed and the result was presented in Fig. 5D. A higher score indicates more severe injury. The scores in the NS and Vehicle groups were significantly higher than those in the Mito group ($P<0.05$), indicating that mitochondrial damage in the Mito group was mitigated by mitochondrial transplantation. In the NS and Vehicle groups, the myocardial myofibrils exhibited a disordered arrangement on TEM, with variation in sarcomeres length and loss of Z-lines. Translucent and swollen mitochondria were visible, exhibiting a larger gap between membranes, distorted cristae, and accumulated calcium. In contrast, the mitochondria sarcomeres of the Mito group were more distinct, and the myocardial myofibrils were arranged in a more orderly fashion. The M-lines and Z-lines were clearly visible, and the number of mitochondrial cristae had increased, with their structure appearing to be complete.

Mitochondrial transplantation improves mitochondrial metabolism of cardiac tissue after CA-CPR. The mitochondrion supplies nearly all of the cell's energy through oxidative phosphorylation, which occurs via the mitochondrial respiratory chain. In instances of global ischemia, there is a deficiency of oxygen available to the mitochondria, which inhibits oxidative phosphorylation (***Rousou, et al.**,**2004***). The activity of mitochondrial complexes II and IV, along with ATP content in cardiac tissue, were assessed in our research to reflect mitochondrial metabolism. Compared with the Sham group, complex II and IV activity and ATP content were significantly attenuated in the other three groups ($P<0.05$). In contrast, the activity of complexes II and IV and ATP content were significantly elevated in the Mito group compared with the NS and Vehicle groups, suggesting that transfer of exogenous mitochondria enhanced function and energy metabolism of resident mitochondria ($P<0.05$, Fig. 5E, 5F, 5G).

Mitochondrial transplantation limits mitochondrial permeability transition pore (mPTP) opening. The opening of the mPTP induces mitochondrial permeability transition, resulting in the uncoupling of oxidative phosphorylation, an increase in mitochondrial volume (swelling), and the dissipation of the mitochondrial membrane potential. Following calcein acetoxymethyl ester (Calcein AM) staining and cobalt chloride (CoCl2) treatment, the opening level of mPTP was assessed using flow cytometry. In this assay, stronger fluorescence intensity indicates lower mPTP opening (Fig. 5H, 5I). The rats in the Mito group demonstrated lower fluorescence intensity, which means a higher mPTP opening level compared with the Sham group. The rats of NS and Vehicle groups showed further increased mPTP opening level compared with the Mito group. Mitochondrial transplantation caused a significant reduction in mitochondrial swelling.

Effects of mitochondrial transplantation on cardiomyocytes.

Mitochondrial transplantation alleviates myocardial oxidative stress injury after CA-CPR. Increased level of reactive oxygen species (ROS) during reperfusion are a critical factor in the development of reperfusion injury. Consequently, oxidative stress in the ischemic myocardium of rats undergoing CA-CPR was evaluated. First, we evaluated the level of ROS in myocardial mitochondria. We used probe DCFH-DA, which releases green fluorescence in response to esterase oxidation, to measure ROS level based on fluorescence intensity. As shown in Fig. 6A, the ROS content in the myocardial mitochondria increased after 4 hours of reperfusion, and decreased with the transplantation of isolated mitochondria. Second, the production of malondialdehyde (MDA), which is widely used as ‘footprints’ of ROS generation, was also monitored. MDA level in the myocardial tissue of rats 4 hours after ROSC was decreased in animals given exogenous mitochondria (Fig. 6B, $P<0.05$). Third, our results indicated that the activity of superoxide dismutase (SOD) was significantly elevated in the Mito group compared with both NS and Vehicle groups (Fig. 6C, $P<0.05$).

Mitochondrial transplantation reduces cardiomyocyte apoptosis. Apoptotic indices and the apoptotic rate, as assessed by the terminal deoxynucleotidyl transferase dUTP nick-end labeling (TUNEL) assay and flow cytometry, increased 4 hours after ROSC. Compared with the NS and Vehicle groups, the apoptotic indices and apoptotic rate in the Mito group were lower ($P<0.05$), which linked exogenous mitochondrial transplantation and cardiomyocyte apoptosis reduction after CPR (Fig. 6D, 6E, 6F). The expression of cleaved caspase-3 protein in the Mito group was lower than that in the NS and Vehicle groups. (Fig. 6G, 6H)

Mitochondrial transplantation reduces the markers of myocardial injury. ELISA was used to detect the expression of myocardial injury markers, Creatine Kinase MB isoenzyme (CK-MB) and Cardiac Troponin I (cTn-I), at 4 hours after ROSC. Compared with the Sham group, the level of CK-MB and cTn-I in the serum of the other three groups showed a significant rise ($P<0.05$). However, both CK-MB and cTn-I level in the serum of the Mito group were lower than those in the NS and Vehicle groups, suggesting that myocardial injury was reduced ($P<0.05$, Fig. 6I, 6J).

Mitochondrial transplantation attenuates myocardial histopathologic changes. Four hours after ROSC, myocardium from each experimental groups were subjected to histological evaluation (Fig. 6K, 6L). Tissue samples from the Sham group exhibited a well-organized structure of myocardial fibers, with no apparent inflammatory cell infiltration into the stroma. In the NS and Vehicle groups, the myocardial fibers were disordered, with some myocardial cells exhibiting thickening, rupture, and vacuolization. Also, there was inflammatory cell invasion in the stroma. The myocardial arrangement in the Mito group was more neatly arranged than that in the NS and Vehicle groups although thickening of myocardial cells was noted.

Discussion

PAMD is a common complication following resuscitated. It is characterized by systolic and diastolic insufficiency, arrhythmias, and recurrent CA. Circulatory dysfunction occurs in approximately two-thirds of CA subjects, which is associated with a poor outcome (***Han and Lee**,**2022***). Unlike myocardial depression caused by regional ischemia characterized by localized ventricular wall-motion abnormalities, myocardial depression caused by PAMD after CA manifest as global left ventricular systolic dysfunction accompanied by reduced ejection fraction, left ventricular diastolic dysfunction, and right ventricular dysfunction (***Lazzarin, et al.**,**2022***; ***Xu, et al.**,**2008***). Of these, global left ventricular systolic dysfunction is the most significant manifestation.

In the present study, we tested the hypothesis that the administration of exogenous mitochondria is cardioprotective effects after CPR. The rationale was to enhance the energy-dependent contractility of the myocardium. We isolated mitochondria from allogeneic gastrocnemius muscle tissue of healthy rats and maintained optimal mitochondrial activity and therapeutic effects. CA is an occasional event, making it impossible to predict when it will occur. Consequently, it is consistent with clinical practice to perform mitochondrial transplantation interventions only after spontaneous circulation has recovered and stabilized. The dosage of mitochondria is determined based on previous studies (***Blitzer, et al.**,**2020***; ***Guariento, et al.**,**2020***). In previous research, isolated mitochondria (1×10^9) were delivered to the left coronary ostium in pigs, and can be a viable treatment in cardiac ischemia-reperfusion injury (***Blitzer, et***

al.**,**2020; ***Guariento, et al.**,**2020***). Additionally, the dose of 1×10^9 mitochondria achieves the maximal hyperemic effect when administered via intracoronary injection (***Shin, et al.**,**2019***). Considering that Sprague-Dawley (SD) rats are smaller than pigs and that there is a loss of mitochondria during pulmonary circulation, we adopted a mitochondrial transplantation dose of 5×10^8. Subsequently, uptake of the delivered mitochondria occurred in the heart and myocytes, perhaps via micropinocytosis (***Kami and Gojo**,**2020***). AS well, mitochondrial internalization occurred through actin-dependent endocytosis (***Pacak, et al.**,**2015***). Internalized mitochondria promote degradation of resident via lysosomes to maintain an energy mitochondrial balance (***Jia, et al.**,**2022***; ***Liu, et al.**,**2022***). Notably, Cowan et al. (***Cowan, et al.**,**2017***) indicated that isolated mitochondria are transported to endosomes and lysosomes; however, most of these mitochondria escape from these compartments and subsequently fuse with the endogenous mitochondrial network. Internalized mitochondria facilitated respiratory restoration in recipient cells with depleted mtDNA, and improved cellular function by increasing ATP level and oxygen-consumption rates (***Pacak, et al.**,**2015***).

In our results, increased numbers of mitochondria were not found in the hearts of treated animals. Possibly because CPR caused ischemia/reperfusion injury to organs throughout the body, with non-specific distribution and uptake of the delivered mitochondria. Moreover, mitochondria possess the ability to adjust their mass and function to maintain cellular homeostasis. This includes mitochondrial dynamics such as fusion and fission, as well as biogenesis and degradation through mitophagy, which are crucial for regulating the morphology, mass, and function of mitochondria (***Quiles and Gustafsson**,**2020***). These mechanisms may regulate the continuous remodeling of mitochondrial numbers to maintain mitochondrial mass homeostasis following mitochondrial transplantation (***Jia, et al.**,**2022***). After mitochondrial transplantation, the energy supply of myocardial mitochondria was restored, and autophagy was enhanced, resulting in an increased clearance of damaged mitochondria (***Xu, et al.**,**2024***). This also clarifies why the overall mass of mitochondria did not increase.

Masuzawa et al. (***Masuzawa, et al.**,**2013***) proposed that the internalization of mitochondria is not critical, as cardioprotection occurs rapidly within 10 minutes of reperfusion, the presence of viable mitochondria in cardiac tissue is all that is required. The nonviable mitochondria, mitochondrial fractions, mitochondrial deoxyribonucleic acid, ribonucleic acid, and exogenous adenosine diphosphate and ATP are incapable of providing protection to the ischemic heart (***Masuzawa, et al.**,**2013***). Shin et al. (***Shin, et al.**,**2019***) also suggested that the number of mitochondria required for cardioprotection is not dependent on the absolute number of transplanted mitochondria. Therefore, an increase in mitochondrial mass may not be the mechanism underlying the cardioprotective effects of transplanted mitochondria. The cardioprotective mechanisms of isolated mitochondria involve increased ATP production. The results of our study were consistent with other date that the energy metabolism of myocardial mitochondria improved after mitochondrial transplantation along with increased complex activity and ATP content (***Jia, et al.**,**2022***; ***Pacak, et al.**,**2015***). Mitochondrial transplantation is being pursued as a therapeutic strategy, as it does not result in coronary occlusion, autoimmunity and arrhythmia attacks (***Masuzawa, et al.**,**2013***; ***Shin, et al.**,**2019***). The clinical application of mitochondrial transplantation can enhance the prognosis of pediatric patients requiring extracorporeal membrane oxygenation following cardiac surgery, the improvement of cardiac function in patients helps them successfully wean off ECMO support (***Emani and McCully**,**2018***). It is worth noting that the method of mitochondrial isolation may better meet the needs of clinical settings where an interventional time below 60 minutes is desired (***Ali, et al.**,**2021***). After the isolation, mitochondria can be immediately used for transfer and internalization (***Ali, et al.**,**2021***). Still concerns regarding mitochondrial hemocompatibility and stability in serum have been raised. In this line, serum calcium did not adversely impact isolated mitochondria (***Maleki, et al.**,**2023***).

ROS is generated with ischemia and then targets the normal physiologic functions of cells by damaging the structures of proteins, lipids, and even DNA (***Zhu, et al.**,**2024***).

As well, oxidative stress promotes cardiac ischemia-reperfusion injury and was implicated in pro-inflammatory responses and apoptosis, both of which worsen myocardial cell injury (***Patel and Karch**,**2020***). In a regional ischemia-reperfusion model, mitochondrial transplantation reduced oxidative stress in cells following reperfusion (***Zhang, et al.**,**2019***). Similarly, in the present study, mitochondrial transplantation reduced the production of ROS, decreased the level of myocardial oxidative markers, and increased the activity of antioxidant enzymes after 4 hours of ROSC.

Ischemia/reperfusion injury of myocardial tissue releases CK-MB and cTn-I, which were commonly used indicators of early myocardial injury in clinical settings (***Zhang, et al.**,**2021***). The concentrations of CK-MB and cTn-I rose significantly 4 hours after resuscitation in the CA-CPR model, while mitochondrial transplantation significantly reduced this effect. During ischemia, the loss of mitochondrial membrane potential leads to mitochondrial swelling and release of cytochrome C, followed by caspase-mediated cell death during reperfusion (***Lu, et al.**,**2023***; ***Milliken, et al.**,**2022***). Apoptosis is the process by which cardiomyocytes die (***Kunapuli, et al.**,**2006***). Increase apoptosis was found in rats after CA-CPR along with increased caspase-3 expression after resuscitation (***Wu, et al.**,**2021***). Similar results were reported in pigs that underwent CA-CPR (***Wang, et al.**,**2023***). In our results, the level of apoptosis and the opening of mPTP in cardiomyocytes increased significantly after CPR, whereas administration of healthy mitochondria significantly reduced both apoptosis and mPTP opening. Moreover, exogenous mitochondrial transplantation significantly reduced the disordering of myocardial fiber arrangement and inflammatory cell infiltration.

In conclusion, exogenous mitochondrial transplantation improved cardiac function after CPR. The specific mechanism involved may be related to the improvement in mitochondrial function, thus reducing the oxidative-stress response and apoptosis of myocardial cells. These dates suggest possible advantage in mitochondrial transplantation following CPR.

Limitations

Hemodynamic observation was carried out only for 4 hours after ROSC, Thus, the impact of mitochondrial transplantation on long-term cardiac function following CPR could not be assessed. In this study, the animal model consisted of healthy rats. However, in clinical practice, CA is primarily caused by cardiac issues. Healthy rats tend to exhibit a higher recovery ability after a CA attack, which may lead to an overestimation of the therapeutic effects of mitochondrial transplantation. In our next phase, we plan to utilize various CA models to conduct comprehensive studies to validate the effectiveness of mitochondrial transplantation in different pathological models.

Methods

Animals

The experimental protocol (Fig.1) was approved by the Animal Experiment Committee of the General Hospital of Central Theater Command (No.2023017) and conformed to the Guide for the Care and Use of Experimental Animals published by the National Institutes of Health, USA (NIH Publication No. 5377-3, 1996). Adult male SD (7 to 8 weeks old) rats weighing 250 to 350g were purchased from Hunan Silaikejingda Experimental Animal Co., Ltd. (No. 430727231102711675, Changsha, China). Male rats were selected to avoid estrous cycle interference. Animals were housed in standard cages with a 12-hour light-dark cycle at a room temperature 22°C.

Animals were randomly assigned to four groups using the random number table method: a Sham group, NS group, Vehicle group, and Mito group (n=17). Each group was further divided into two survival-analysis subgroups: a four-hour group (n=7) and a 72-hour group (n=10). Rats in the NS, Vehicle and Mito groups underwent CA induced by asphyxia and CPR, while rats in the Sham group underwent tracheal intubation and arteriovenous puncture only, without CA and CPR.

Experimental protocol

CA-CPR model Establishment of the CA-CPR model was as previously published (***Huang, et al.***,***2020***). Rats were anesthetized with pentobarbital sodium (45 mg/kg) via intraperitoneal injection. A 16-G intravenous catheter was used for endotracheal intubation. The left femoral artery and right femoral vein were subsequently inserted using a 24-G venous indwelling needle for dynamic blood pressure detection and venous access establishment. Blood pressure, HR, and rectal temperature were monitored using the ALC-MPA monitoring system (Alcott Biotech, Shanghai, China). After 10 minutes of mechanical ventilation, asphyxia-mediated CA was induced by blocking the tracheal tube. CA was defined as a decrease in systolic blood pressure to 25 mmHg. Five minutes after CA, external chest compression (200 bpm) and mechanical ventilation (tidal volume, 0.60 mL/100 g, respiratory rate, 80 bpm) were initiated, and epinephrine (40 mcg/kg) was administered intravenously. ROSC was defined as the spontaneous restoration of sinus rhythm with a systolic blood pressure of >60 mmHg that was maintained for 10 minutes. Subsequently, corresponding treatments were administered. Animals that did not regain autonomic circulation within 5 minutes were excluded from the study. After ROSC, hemodynamics and echocardiograms were recorded for 4 hours. Basal body temperature was maintained at 37°C throughout the intervention. Pentobarbital sodium (10 mg/kg) was given if animals urinated or showed increased limb-muscle tension. Twenty-eight animals of 4-hour group completed the full protocol and were humanely euthanized with excess pentobarbital sodium 4 hours after ROSC. Myocardial tissue and blood samples were collected for detection. The remaining 40 animals of 72-hour group were monitored for 72-hour to track survival.

Intervention measures Ten minutes after ROSC, 0.5 mL of normal saline, 0.5 mL of respiration buffer, and 0.5 mL of 1×10^9/mL mitochondrial suspension were injected through the femoral vein in the NS, Vehicle, and Mito groups, The Sham group received 0.5 mL of NS at 30 minutes postoperatively.

Echocardiography

To assess myocardial function, an ultra-high resolution, small-animal ultrasound imaging system (SigmaVET, Esaote, Genoa, Italy) was used to capture M-mode echocardiographic images at the parasternal long axis and/or parasternal short axis near the papillary muscle at 1-hour, 2-hour, 3-hour, and 4-hour post-ROSC.

Survival analysis

In the 72-hour survival study cohort, the catheters were extracted 4 hours post-ROSC, and the surgical incisions were closed. Animals were placed back in their cages and administered subcutaneous injections of 0.5mL of 1% lidocaine for analgesia. Animals were monitored every 2 hours during the initial 24 hours following ROSC, and then at 48 and 72 hours. Animals that exhibited signs such as wheezing or a respiratory rate below 5 breaths per minute were deemed moribund and humanely euthanized (***Su, et al.**,**2021***). At the end of the time rats were euthanized.

Isolation and identification of mitochondria

Mitochondrial isolation and labeling Mitochondria were isolated as published (***Preble, et al.**,**2014***). In brief, 180 mg of gastrocnemius muscle from healthy male SD rats aged 7 to 8 weeks were placed into a centrifuge tube containing 5 mL of pre-chilled homogenizing buffer (300 mM sucrose, 10 mM K-HEPES, and 1 mM K-EGTA), homogenized, and incubated on ice with *Bacillus subtilis,* a protease (P5380, Sigma Aldrich, Darmstadt, Germany), for 10 minutes. The mixture was filtered through a 40-μm cell filter, and then bovine serum albumin (ST023-50 g, Beyotime, Shanghai, China) was added and incubated for 5 minutes. The homogenate was then filtered through a 40-μm screen and then through a 10-μm screen, and centrifuged at 9000 g for 10 minutes at 4℃. The precipitate was reconstituted in 1 mL of pre-chilled respiration buffer (250 mM sucrose, 2 mM potassium dihydrogen phosphate, 10 mM magnesium chloride, 20 mM K-HEPES, and 0.5 mM K-EGTA). Mitochondrial amounts were determined as previously published and were quantified using a bacterial counter (0650010, Marienfeld, Lauda-Königshofen, Germany) (***McCully, et al.***,***2009***). The isolated mitochondria were incubated with Mito-Tracker Red CMXRos (C1049B-50μg, Beyotime, Shanghai, China) at 37□ for 15 minutes and then washed three times with the mitochondrial respiration buffer.

Detection of mitochondrial membrane potential A mitochondrial membrane potential detection kit (JC-1) (C2003S; Beyotime, Shanghai, China) was used to characterize function. Purified mitochondria were incubated with JC-1 staining solution at 37°C for 20 minutes, followed by imaging with a fluorescence microscope (BX53, OLYMPUS, Tokyo, Japan) equipped with a WHN 10/22 eyepiece. The image analysis software used was OLYMPUS cellSens Standard version 3.2.

Western blotting Tissue samples and isolated mitochondria were lysed in RIPA buffer (P0013B; Beyotime, Shanghai, China) containing 1% PMSF (ST505; Beyotime, Shanghai, China) on ice to extract proteins. Protein concentration was determined by the BCA method. Protein was boiled in a water bath for 10 minutes. Electrophoresis was performed using a 12% SDS-PAGE gel (P0012A, Beyotime, Shanghai, China), followed by transfer to a PVDF membrane (FFP70, Beyotime, Shanghai, China). Non-specific binding was blocked with 5% skim milk powder at room temperature for 2 hours. Membranes were exposed to primary antibodies overnight at 4□: anti-Caspase-3 (1:1000, 14220T, Cell Signaling Technology, Beverly, MA, USA), anti-TOM20 (1:1000, AF5206; Affinity, Changzhou, China), anti-COX □ (1:1000; AC610, Beyotime, Shanghai, China) and anti-GAPDH (1:3000; LF206, Epizyme, Shanghai, China) on a shaker at 4□ for 12 hours. After washing, membranes were incubated with horseradish peroxidase-labeled secondary antibody (1:2000, A0208, Beyotime, Shanghai, China) for 2 hours and developed with the ECL chemiluminescence method. Results from immunoblots were scanned using the chemiluminescence imaging system (SH-523, Shenhua, Hangzhou, China; JY-Clear ECL, JUNYI, Beijing, China;). The relative band intensities were quantified using ImageJ software (version 1.54f; National Institutes of Health, USA).

Mitochondrial distribution and uptake

Mitochondrial co-localization was determined as published (***Masuzawa, et al.,2013***). Tissue sections were incubated with 0.25% Triton-X-100 for 10 minutes at room temperature, blocked with normal bovine serum albumin, and incubated with primary antibody generated against alpha-actinin 2 (1:500; GTX103219; GeneTex, Irvine, USA) at 4℃ overnight. After washing with PBST, sections were incubated with an Alexa Fluor 488-labeled secondary antibody (1:1000, HZ0176; Huzhen, Shanghai, China) for 1 hour. DAPI (P0131-5 ml; Beyotime, Shanghai, China) was applied to stain nuclei. Images were acquired using the OLYMPUS fluorescence microscope.

Analysis of cardiac mitochondria

Complex activity Mitochondria were extracted from 0.1 g myocardial tissue using differential centrifugation. The mitochondrial suspension was disrupted by ultrasonic waves in an ice bath releasing the mitochondrial respiratory chain complex. The working solution from mitochondrial complex activity test kit (AKOP008M, AKOP006M; Boxbio, Beijing, China) was mixed with the samples and the absorbance at 605 nm and 550 nm measured values at various timepoints. The variance between the two timepoints was calculated and recorded as $\Delta A1$ and $\Delta A2$. Protein concentration (C) of each sample was measured. Mitochondrial complex II activity was calculated as $476.19 \times \Delta A1/C$, and mitochondrial complex IV activity was calculated as $1099.48 \times \Delta A2/C$.

ATP determination ATP level was determined using an ATP-content test kit (A095-1-1; Nanjing Jiancheng, Nanjing, China).

TOM20 labeling Tissue sections were labeled with TOM20 antibody (1:100, AF5206; Affinity, Changzhou, China), incubated with a horseradish peroxidase-coupled secondary antibody (1:400, 5220-0336; SeraCare, Massachusetts, USA), subjected to tyramide signal amplification (TSA), stained with DAPI and images acquired using an OLYMPUS fluorescence microscope.

Transmission electron microscope Fixed hearts were rinsed with phosphate-buffered saline (PBS) for 45 minutes and exposed to 1% osmium tetroxide for 2 hours. After dehydration in graded ethanol concentrations, tissue samples were immersed in epoxy resin, embedded, and cut into ultrathin sections (60-80 nm). The sections were stained with uranium and lead, and examined and imaged using a TEM (HT7800; Hitachi, Tokyo, Japan). The degree of mitochondrial damage in the 4 groups was assessed using the Flameng classification method. The evaluation is conducted by trained experimenters who are unaware of the group assignments. Mitochondrial damage was evaluated on a scale from 0 to 4, where 0 indicates a normal structure, 1 indicates normal with slight swelling, 2 indicates mitochondrial swelling, 3 indicates serious swelling and cristae disorder, 4 indicates mitochondria membrane breach and vacuolization. Based on this scale, the degree of mitochondrial damage in rats across the four groups was scored, and the average scores were calculated from three random fields of view per rat. A higher score indicates more severe injury (***Zhang, et al.***,***2017***).

The determination of ROS The extraction of mitochondria from myocardial tissue was performed using a mitochondrial isolation kit (S3606; Beyotime, Shanghai, China). Rat myocardial tissues were homogenized with mitochondrial isolation reagent A and then centrifuged at 600 g for 5 minutes at 4°C. The supernatant was subsequently centrifuged again at 11,000 g for 5 minutes at 4°C. ROS was determined by a fluorescent probe DCFH-DA using the ROS assay kit (S0033S; Beyotime, Shanghai, China) based on the manufacturer’s directions. After removing the supernatant, the pelleted materials were suspended in incubation buffer (20 mM

MOPS, 0.1 M KCl, 10 mM ATP, 10 mM $MgCl_2$, 10 mM sodium succinate, and 1 mM EGTA); then DCFH-DA (1: 1000) was added. Next, the contents were mixed and incubated at 37°C in the dark for 20 minutes. Finally, the fluorescence intensity was measured on a flow cytometry with excitation and emission wavelengths of 485 nm and 525 nm, respectively. The results were presented as the fluorescent intensity per nanogram of protein.

Quantification of MDA and SOD detection The MDA and SOD activity level of myocardial samples were determined with an MDA test kit (A003-1; Nanjing Jiancheng, Nanjing, China) and SOD test kit (A001-3; Nanjing Jiancheng, Nanjing, China).

Mitochondrial swelling assay Myocardial tissue was initially isolated. The tissue was digested using 0.1% collagenase and 0.125% trypsin, followed by hydrolysis at 37℃ for 30 minutes. The mixture was filtered through a 200-mesh screen at 1,500 rpm and then centrifuged for 15 minutes to collect the sediment. mPTP Assay Kit (C2009S; Beyotime, Shanghai, China) was used to determine the opening of the mPTP in cardiomyocytes. This kit provides a more straightforward approach for assessing mPTP opening. In brief, cardiomyocytes were treated with Calcein AM for 30 minutes at 37℃, which easily entered the cells and accumulated in various cytosolic compartments, including the mitochondria. Once inside, intracellular esterases broke down the acetoxymethyl esters, releasing the highly polar fluorescent dye calcein. The fluorescence from cytosolic calcein was diminished when CoCl2 was added, while the fluorescence from mitochondrial calcein remained unaffected. However, when the mPTP opened, mitochondrial calcein was released into the cytosol, where it was quenched by CoCl2, leading to a notable decrease in calcein fluorescence. A decrease in absorbance reflects mitochondrial swelling and the opening of the mitochondrial mPTP. Subsequently, flow cytometry was employed to detect the opening of the mPTP in 1×10^6 cardiomyocytes.

Detection of myocardial injury

TUNEL assay Paraffin-embedded tissue sections were processed with an *in-situ* cell-death detection kit (11684795910; Roche, Basel, Switzerland) for terminal deoxynucleotidyl transferase-mediated deoxyuridine triphosphate nick-end labeling. The ratio of TUNEL-positive cells to total cells was determined.

Flow cytometry To prepare a single-cell suspension, the separation of cardiomyocytes is described as previously mentioned. Cells were washed with PBS, suspended in the binding buffer (from Annexin V-FITC/PI apoptosis detection kit below-mentioned) and stained with AnnexinV-FITC and PI (Annexin V-FITC/PI apoptosis detection kit; A211-02; Vazyme, Nanjing, China). Apoptosis was assessed using flow cytometry.

Markers of ischemic injury Blood samples were collected from the femoral artery and centrifuged for 15 minutes at 3000 rpm to obtain serum. The level of myocardial-injury markers was measured using the CK-MB kit (MM-0625R1; Meimian, Yancheng, China) and the cTn-I kit (MM-0426R2; Meimian, Yancheng, China).

Histology Hearts was fixed in 4% paraformaldehyde for 24 hours, dehydrated, rendered transparent, embedded in paraffin and cut into thin sections. After dewaxing and rehydration, the sections were stained with hematoxylin and eosin, and images acquired using a light microscope. A histological score was utilized to evaluate the extent of myocardial injury, based on the criteria established by Rona et al. (***RONA, et al.***,***1959***). (Supplemental Table1).

Statistics and data analysis

IBM SPSS Statistics software (V26.0, IBM Corp, New York, USA) was used for data analysis. All data are expressed as mean ± standard deviation (Mean ± SD). Sample size for the 4-hour group was calculated as published (***Dell, et al.***,***2002***). The ejection fraction of the first three surviving rats among the groups was measured. The population standard deviation of the variable is 11.34. With a magnitude of difference set at 15, an error rate of 0.1, and a power of 80%, the smallest acceptable sample size was determined to be five animals. Considering an animal loss of approximately 20% after 4 hours of CPR, seven animals were selected for each group. The sample size for the 72-hour group was calculated using StatBox (StatBox-Open 0.1.0; Cloud Powered Clinical Trial, Hebei, China). Set the survival rate at 20% for survival rate 1 and 80% for survival rate 2 (with power = 0.8 and α = 0.05). Accordingly, 10 was the smallest acceptable animal sample size. The comparison of time-based measurements was evaluated using repeated-measures tow-way ANOVA, with groups as the between-subjects factor and time as the within-subjects factor. One-way ANOVA and Tukey's multiple-comparison test were employed to compare multiple groups. Survival was characterized using the Kaplan-Meier survival analysis test. Statistical significance was defined at $P<0.05$.

Acknowledgments

We thank LetPub (www.letpub.com) for linguistic assistance and presubmission expert review.

Additional information

Funding

This work was supported by the National Natural Science Foundation of China (82372210, 81901932) and Natural Science Foundation of Hubei Province (2021CFB492).

Author contributions

X.Z. and G.S.G. supervised the study and designed the experiments. Z.W. and J.Z performed the experiments. Z.W and J.Z. collected, analyzed and interpreted the data. M.D.X. and J.Y.Y. supervised the experiments. X.Y.M. and M.Z.S. accessed and verified the data. Z.W. and J.Z. wrote the manuscript. X.Z. and G.S.G. revised the manuscript. All authors read and approved the final version of the manuscript.

Ethics

The animal experiments were approved by the Animal Experiment Committee of the General Hospital of Central Theater Command (No.2023017).

Additional files

Supplementary files

Supplementary Table S1. Details of antibodies used in the methodology.

Supplementary Table S2. Scoring standard of myocardial pathological injury.

Supplementary Figure 1. Localization and uptake of transplanted mitochondria in myocardium and epicardium.

Data availability

The data underlying this article will be shared on reasonable request to the corresponding author.

References:

Abrigo J, Olguín H, Tacchi F, Orozco-Aguilar J, Valero-Breton M, Soto J, Castro-Sepúlveda M, Elorza AA, Simon F, Cabello-Verrugio C. 2023. Cholic and deoxycholic acids induce mitochondrial dysfunction, impaired biogenesis and autophagic flux in skeletal muscle cells. *BIOL RES* 56:30. doi:10.1186/s40659-023-00436-3

Ali PP, Hosseinian S, Kheradvar A. 2021. Mitochondrial transplantation in cardiomyocytes: foundation, methods, and outcomes. *AM J PHYSIOL-CELL PH* 321:C489-C503. doi:10.1152/ajpcell.00152.2021

Blitzer D, Guariento A, Doulamis IP, Shin B, Moskowitzova K, Barbieri GR, Orfany A, Del NP, McCully JD. 2020. Delayed Transplantation of Autologous Mitochondria for Cardioprotection in a Porcine Model. *ANN THORAC SURG* 109:711-719. doi: 10.1016/j.athoracsur.2019.06.075

Cao X, Yao F, Zhang B, Sun X. 2023. Mitochondrial dysfunction in heart diseases: Potential therapeutic effects of Panax ginseng. *FRONT PHARMACOL* 14:1218803. doi:10.3389/fphar.2023.1218803

Cowan DB, Yao R, Thedsanamoorthy JK, Zurakowski D, Del NP, McCully JD. 2017. Transit and integration of extracellular mitochondria in human heart cells. *SCI REP-UK* 7:17450. doi:10.1038/s41598-017-17813-0

Dell RB, Holleran S, Ramakrishnan R. 2002. Sample size determination. *ILAR J* 43:207-213. doi:10.1093/ilar.43.4.207

Emani SM, McCully JD. 2018. Mitochondrial transplantation: applications for pediatric patients with congenital heart disease. *TRANSL PEDIATR* 7:169-175. doi:10.21037/tp.2018.02.02

Gazmuri RJ, Radhakrishnan J. 2012. Protecting mitochondrial bioenergetic function during resuscitation from cardiac arrest. *CRIT CARE CLIN* 28:245-270. doi: 10.1016/j.ccc.2012.02.001

Guariento A, Blitzer D, Doulamis I, Shin B, Moskowitzova K, Orfany A, Ramirez-Barbieri G, Staffa SJ, Zurakowski D, Del NP, McCully JD. 2020. Preischemic autologous mitochondrial transplantation by intracoronary injection for myocardial protection. *J THORAC CARDIOV SUR* 160: e15-e29. doi: 10.1016/j.jtcvs.2019.06.111

Hall AR, Burke N, Dongworth RK, Hausenloy DJ. 2014. Mitochondrial fusion and fission proteins: novel therapeutic targets for combating cardiovascular disease. *BRIT J PHARMACOL* 171:1890-1906. doi:10.1111/bph.12516

Han C, Lee JH. 2022. Heart rate and diastolic arterial pressure in cardiac arrest patients: A nationwide, multicenter prospective registry. *PLOS ONE* 17: e274130. doi: 10.1371/journal.pone.0274130

Huang CH, Tsai MS, Chiang CY, Su YJ, Wang TD, Chang WT, Chen HW, Chen WJ.

2015. Activation of mitochondrial STAT-3 and reduced mitochondria damage during hypothermia treatment for post-cardiac arrest myocardial dysfunction. *BASIC RES CARDIOL* 110:59. doi:10.1007/s00395-015-0516-3

Huang Y, Gao X, Zhou X, Xie B, Zhang Y, Zhu J, Zhu S. 2020. Mitophagy in the Hippocampus Is Excessive Activated After Cardiac Arrest and Cardiopulmonary Resuscitation. *NEUROCHEM RES* 45:322-330. doi:10.1007/s11064-019-02916-z

Jia L, Yang L, Tian Y, Yang L, Wu D, Zhang H, Li M, Wu N. 2022. Nrf2 participates in the protective effect of exogenous mitochondria against mitochondrial dysfunction in myocardial ischaemic and hypoxic injury. *CELL SIGNAL* 92:110266. doi: 10.1016/j.cellsig.2022.110266

Kami D, Gojo S. 2020. From Cell Entry to Engraftment of Exogenous Mitochondria. *INT J MOL SCI* 21doi:10.3390/ijms21144995

Kunapuli S, Rosanio S, Schwarz ER. 2006. "How do cardiomyocytes die?" apoptosis and autophagic cell death in cardiac myocytes. *J CARD FAIL* 12:381-391. doi: 10.1016/j.cardfail.2006.02.002

Kuwada Y, Takenaka K. 2000. [Transmural heterogeneity of the left ventricular wall: subendocardial layer and subepicardial layer]. *J CARDIOL* 35:205-218.

Lazzarin T, Tonon CR, Martins D, Fávero EJ, Baumgratz TD, Pereira F, Pinheiro VR, Ballarin RS, Queiroz D, Azevedo PS, Polegato BF, Okoshi MP, Zornoff L, Rupp DPS, Minicucci MF. 2022. Post-Cardiac Arrest: Mechanisms, Management, and Future Perspectives. *J CLIN MED* 12doi:10.3390/jcm12010259

Liu Z, Sun Y, Qi Z, Cao L, Ding S. 2022. Mitochondrial transfer/transplantation: an emerging therapeutic approach for multiple diseases. *CELL BIOSCI* 12:66. doi:10.1186/s13578-022-00805-7

Lu CH, Chen DX, Dong K, Wu YJ, Na N, Wen H, Hu YS, Liang YY, Wu SY, Lin BY, Huang F, Zeng ZY. 2023. Inhibition of miR-143-3p alleviates myocardial ischemia reperfusion injury via limiting mitochondria-mediated apoptosis. *BIOL CHEM* 404:619-631. doi:10.1515/hsz-2022-0334

Maleki F, Rabbani S, Shirkoohi R, Rezaei M. 2023. Allogeneic mitochondrial transplantation ameliorates cardiac dysfunction due to doxorubicin: An in vivo study.

BIOMED PHARMACOTHER 168:115651. doi: 10.1016/j.biopha.2023.115651

Masuzawa A, Black KM, Pacak CA, Ericsson M, Barnett RJ, Drumm C, Seth P, Bloch DB, Levitsky S, Cowan DB, McCully JD. 2013. Transplantation of autologously derived mitochondria protects the heart from ischemia-reperfusion injury. *AM J PHYSIOL-HEART C* 304:H966-H982. doi:10.1152/ajpheart.00883.2012

McCully JD, Cowan DB, Pacak CA, Toumpoulis IK, Dayalan H, Levitsky S. 2009. Injection of isolated mitochondria during early reperfusion for cardioprotection. *AM J PHYSIOL-HEART C* 296:H94-H105. doi:10.1152/ajpheart.00567.2008

McCully JD, Del NP, Emani SM. 2023. Mitochondrial transplantation: the advance to therapeutic application and molecular modulation. *FRONT CARDIOVASC MED* 10:1268814. doi:10.3389/fcvm.2023.1268814

Milliken AS, Nadtochiy SM, Brookes PS. 2022. Inhibiting Succinate Release Worsens Cardiac Reperfusion Injury by Enhancing Mitochondrial Reactive Oxygen Species Generation. *J AM HEART ASSOC* 11: e26135. doi:10.1161/JAHA.122.026135

Pacak CA, Preble JM, Kondo H, Seibel P, Levitsky S, Del NP, Cowan DB, McCully JD. 2015. Actin-dependent mitochondrial internalization in cardiomyocytes: evidence for rescue of mitochondrial function. *BIOL OPEN* 4:622-626. doi:10.1242/bio.201511478

Patel P, Karch J. 2020. Regulation of cell death in the cardiovascular system. *INT REV CEL MOL BIO* 353:153-209. doi: 10.1016/bs.ircmb.2019.11.005

Preble JM, Pacak CA, Kondo H, MacKay AA, Cowan DB, McCully JD. 2014. Rapid isolation and purification of mitochondria for transplantation by tissue dissociation and differential filtration. *JOVE-J VIS EXP*: e51682. doi:10.3791/51682

Quiles JM, Gustafsson ÅB. 2020. Mitochondrial Quality Control and Cellular Proteostasis: Two Sides of the Same Coin. *FRONT PHYSIOL* 11:515. doi:10.3389/fphys.2020.00515

RONA G, CHAPPEL CI, BALAZS T, GAUDRY R. 1959. An infarct-like myocardial lesion and other toxic manifestations produced by isoproterenol in the rat. *AMA Arch Pathol* 67:443-455.

Rousou AJ, Ericsson M, Federman M, Levitsky S, McCully JD. 2004. Opening of mitochondrial KATP channels enhances cardioprotection through the modulation of mitochondrial matrix volume, calcium accumulation, and respiration. *AM J PHYSIOL-HEART C* 287:H1967-H1976. doi:10.1152/ajpheart.00338.2004

Shin B, Saeed MY, Esch JJ, Guariento A, Blitzer D, Moskowitzova K, Ramirez-Barbieri G, Orfany A, Thedsanamoorthy JK, Cowan DB, Inkster JA, Snay ER, Staffa SJ, Packard AB, Zurakowski D, Del NP, McCully JD. 2019. A Novel Biological Strategy for Myocardial Protection by Intracoronary Delivery of Mitochondria: Safety and Efficacy. *JACC-BASIC TRANSL SC* 4:871-888. doi: 10.1016/j.jacbts.2019.08.007

Su C, Fan X, Xu F, Wang J, Chen Y. 2021. Prostaglandin E1 attenuates post□cardiac arrest myocardial dysfunction through inhibition of mitochondria□mediated cardiomyocyte apoptosis. *MOL MED REP* 23doi:10.3892/mmr.2020.11749

Tsai MS, Huang CH, Wang CH, Cheng HJ, Wu SN, Chang WT, Chen WJ. 2021. Post-Cardiac Arrest Hydrocortisone Use Ameliorates Cardiac Mitochondrial Injury in a Male Rat Model of Ventricular Fibrillation Cardiac Arrest. *J AM HEART ASSOC* 10:e19837. doi:10.1161/JAHA.120.019837

Wang D, Wang L, Sun Y, Kong F, Jiang Y, An M, Xia Y, Gong P, Yang Y. 2023. Effects of temperature control on hyperthermia-related cardiac dysfunction in a porcine model of cardiac arrest. *CRYOBIOLOGY* 110:49-55. doi: 10.1016/j.cryobiol.2022.12.017

Wu J, Chen H, Qin J, Chen N, Lu S, Jin J, Li Y. 2021. Baicalin Improves Cardiac Outcome and Survival by Suppressing Drp1-Mediated Mitochondrial Fission after Cardiac Arrest-Induced Myocardial Damage. *OXID MED CELL LONGEV* 2021:8865762. doi:10.1155/2021/8865762

Xu M, Zhu J, Wang Z, Yan J, Zhou X. 2024. Neuroprotective effect of autologous mitochondrial transplantation against global ischemia/reperfusion injury in a rat model of cardiac arrest. *MITOCHONDRION* 78:101924. doi: 10.1016/j.mito.2024.101924

Xu T, Tang W, Ristagno G, Wang H, Sun S, Weil MH. 2008. Postresuscitation myocardial diastolic dysfunction following prolonged ventricular fibrillation and cardiopulmonary resuscitation. *CRIT CARE MED* 36:188-192. doi: 10.1097/01.CCM.0000295595.72955.7C

Zhang GR, Peng CM, Liu ZZ, Leng YF. 2021. The effect of dexmedetomidine on myocardial ischemia/reperfusion injury in patients undergoing cardiac surgery with cardiopulmonary bypass: a meta-analysis. *EUR REV MED PHARMACO* 25:7409-7417. doi:10.26355/eurrev_202112_27438

Zhang Y, Hou Y, Wang X, Ping J, Ma Z, Suo C, Lei Z, Li X, Zhang Z, Jia C, Su J. 2017. The effects of kisspeptin-10 on serum metabolism and myocardium in rats. *PLOS ONE* 12: e179164. doi: 10.1371/journal.pone.0179164

Zhang Z, Ma Z, Yan C, Pu K, Wu M, Bai J, Li Y, Wang Q. 2019. Muscle-derived autologous mitochondrial transplantation: A novel strategy for treating cerebral ischemic injury. *BEHAV BRAIN RES* 356:322-331. doi: 10.1016/j.bbr.2018.09.005

Zhu Y, Wang K, Jia X, Fu C, Yu H, Wang Y. 2024. Antioxidant peptides, the guardian of life from oxidative stress. *MED RES REV* 44:275-364. doi:10.1002/med.21986

Table 1 Baseline characteristics of rats and resuscitation characteristics ($\bar{x} \pm s$)

Variable	**n**	**Weight (g)**	**Temp (°C)**	**CA-induced time (sec)**	**CPR time (sec)**	**Adrenaline (mcg)**	**Pentobarbital sodium (mg)**
Sham	17	321.89±14.09	37.20±0.36	-	-	-	22.82±2.01
NS	17	318.65±10.00	37.45±0.43	234.29±22.89	128.41±12.50	12.75±0.40	21.63±1.35
Vehicle	17	326.80±11.64	37.33±0.37	247.06±23.61	138.82±14.64	13.07±0.47	21.79±0.98
Mito	17	320.64±14.32	37.45±0.39	241.29±23.38	131.88±14.51	12.83±0.57	21.92±1.05
***P*-Value**		0.29	0.21	0.57	0.10	0.13	0.07

n = 17 animals per group. CA, cardiac arrest; CPR, cardiopulmonary resuscitation. All data are expressed as Mean ± SD.

Figure 1. Experimental design of the *in-vivo* study, Rats in all groups except the Sham group underwent cardiac arrest for 5 minutes and then received the corresponding intervention 10 minutes after ROSC. Four hours after ROSC, the 4-hour group was used to collect myocardial tissue and blood samples for detection, while the 72-hour group was used for survival detection. BL, baseline; CA, cardiac arrest; ROSC, return of spontaneous circulation.

Figure 2. Observational results at 4 and 72 hours after cardiopulmonary resuscitation in rats. (A) Echocardiograms of rats in each group from baseline to 4 hours following ROSC (n=7). (B) EF of rats in each group from baseline to 4 hours following ROSC (n=7). (C) HR and MAP changes during post -ROSC in 4 hours (n=7). (D) Survival rate during the first 72 hours following ROSC (n=10). Myocardial function between groups was compared by time-based measurements in each group using repeated-measures ANOVA. The survival rate between groups was compared by the Kaplan-Meier survival analysis test. * $P<0.05$ vs. the Sham group and # $P<0.05$ vs. the Mito group. BL, baseline; EF, ejection fraction; HR, heart rate; MAP, mean arterial pressure; bpm, beats per minute; mmHg, millimeters of mercury; AMV, after mechanical ventilation; ROSC, return of spontaneous circulation.

Figure 3. Assessment of the viability and purity of isolated mitochondria. (A) JC-1 staining of mitochondria after isolation from muscle. The staining of isolated mitochondria by JC-1 is visible either as red for J-aggregates or green for J-monomers. The intensity of the red color indicates that the isolated mitochondria had a high membrane potential, confirming their quality for transplantation. Scale bar = 100 μm. (B) SDS/PAGE analysis of fractions obtained during the purification of muscle mitochondria. GAPDH is only expressed in muscle, confirming its purity for transplantation.

Figure 4. Localization and uptake of transplanted mitochondria in endocardium, myocardial tissue was stained for anti-α-actinin 2 (ACTN2; green) and nuclei (blue); the pre-stained isolated mitochondria were labeled red (n=3). Scale bar = 80 μm.

Figure 5. Administration of mitochondria ameliorates ischemia reperfusion-mediated mitochondrial alterations in cardiomyocytes four hours after ROSC. (A and B) A and B represent the detection of fluorescence intensity of TOM20. A represents the image, while B represents the quantitative data. Scale bar = 100 μm (n = 3). (C and D) C shows representative photographs of mitochondrial morphology obtained through TEM examination, with arrows indicate calcium accumulation. D illustrates the degree of mitochondrial damage (n=3). Scale bars = 500 nm. (E and F) Changes in myocardial mitochondrial complex II and IV enzyme activities in hearts (n=7). (G) The ATP content in myocardial tissue was measured by colorimetry (n=7). (H and I) mPTP opening was detected by Calcein staining. I represent the quantitative analysis of the mean fluorescent intensity acquired in H (n = 3). Analyses were performed using ANOVA with Tukey's post hoc test. mPTP opening detection between groups was compared by time-based measurements in each group using repeated-measures ANOVA. The data were expressed as the mean ± standard deviation (SD). * $P<0.05$ vs. the Sham group and # $P<0.05$ vs. the Mito group.

Figure 6. Mitochondrial transplantation reduces myocardial damage 4 hours after ROSC. (A) Detection of mitochondrial ROS in various groups (n=3). (B and C) Changes in malondialdehyde and superoxide dismutase activity level in cardiac tissue (n=7). (D) Myocardial apoptosis level was examined using TUNEL (n=3). Scale bar = 100 μm. (E) The percentage of myocardial apoptosis was examined using flow cytometry (n=3). (F) Quantitative analysis of myocardial TUNEL apoptosis index and flow apoptosis rate (n=3). (G and H) Immunoblotting and quantitative analysis of the expression level of cleaved caspase-3 in the myocardium 4 hours after ROSC (n=3).

(I and J) The changes in CK-MB and cTn-I level in the serum of rats were examined using ELISA (n=7). (K and L) Representative histological sections of the myocardium stained with hematoxylin and eosin. Myocardium from each experimental group were subjected to histological evaluation (n=3), Scale bar = 100 µm. Analyses were performed using ANOVA with Tukey's post hoc test. The data were expressed as mean ± standard deviation (SD). * $P < 0.05$ vs. Sham group and # $P < 0.05$ vs. Mito group. CK-MB, creatine kinase-MB fraction; cTn-I: cardiac troponin-I.

Figure 7. Exogenous mitochondrial transplantation improved cardiac function after CPR. The specific mechanism involved may be related to the improvement in mitochondrial function, thus reducing the oxidative-stress response and apoptosis of myocardial cells. These dates suggest possible advantage in mitochondrial transplantation following CPR.

Supplementary Figure 1. Localization and uptake of transplanted mitochondria in myocardium and epicardium, myocardial tissue was stained for anti-α-actinin 2 (ACTN2; green) and nuclei (blue); the pre-stained isolated mitochondria were labeled red (n=3). Scale bar = 20 µm.

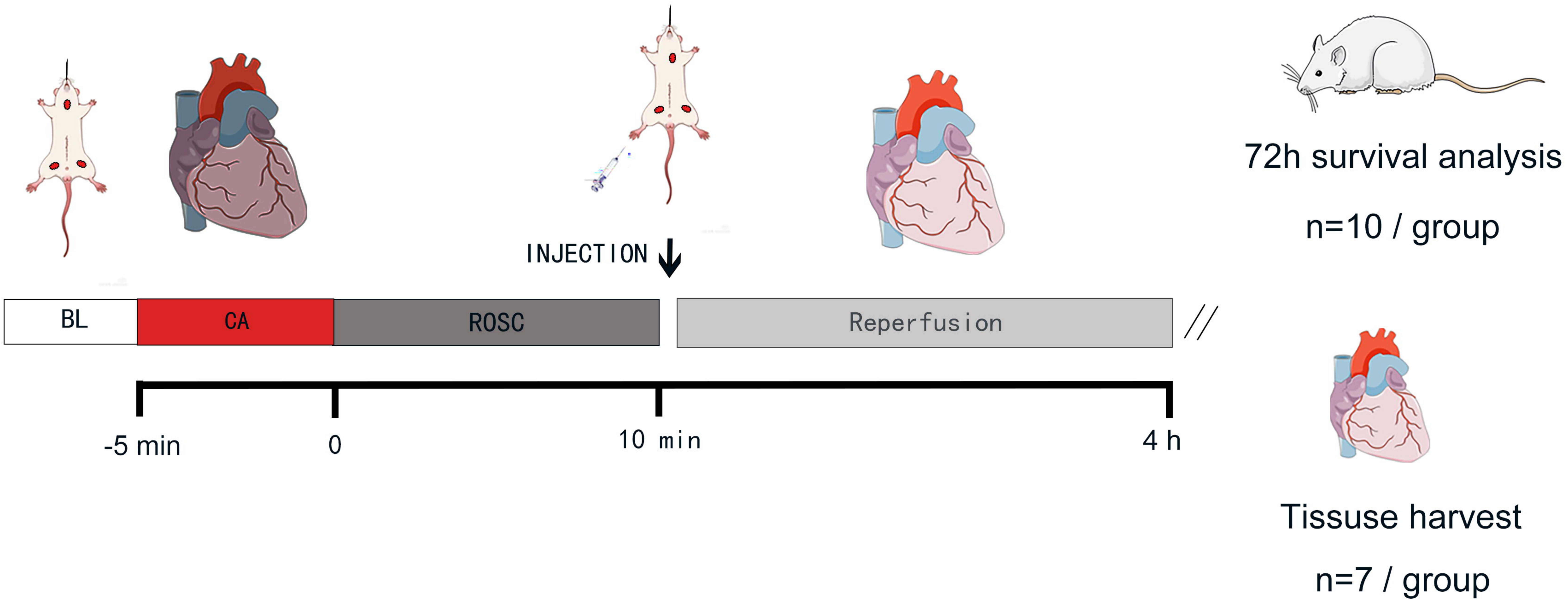
INJECTION
BL
CA
ROSC
Reperfusion
-5 min
0
10 min
4 h
72h survival analysis
n=10 / group
Tissuse harvest
n=7 / group

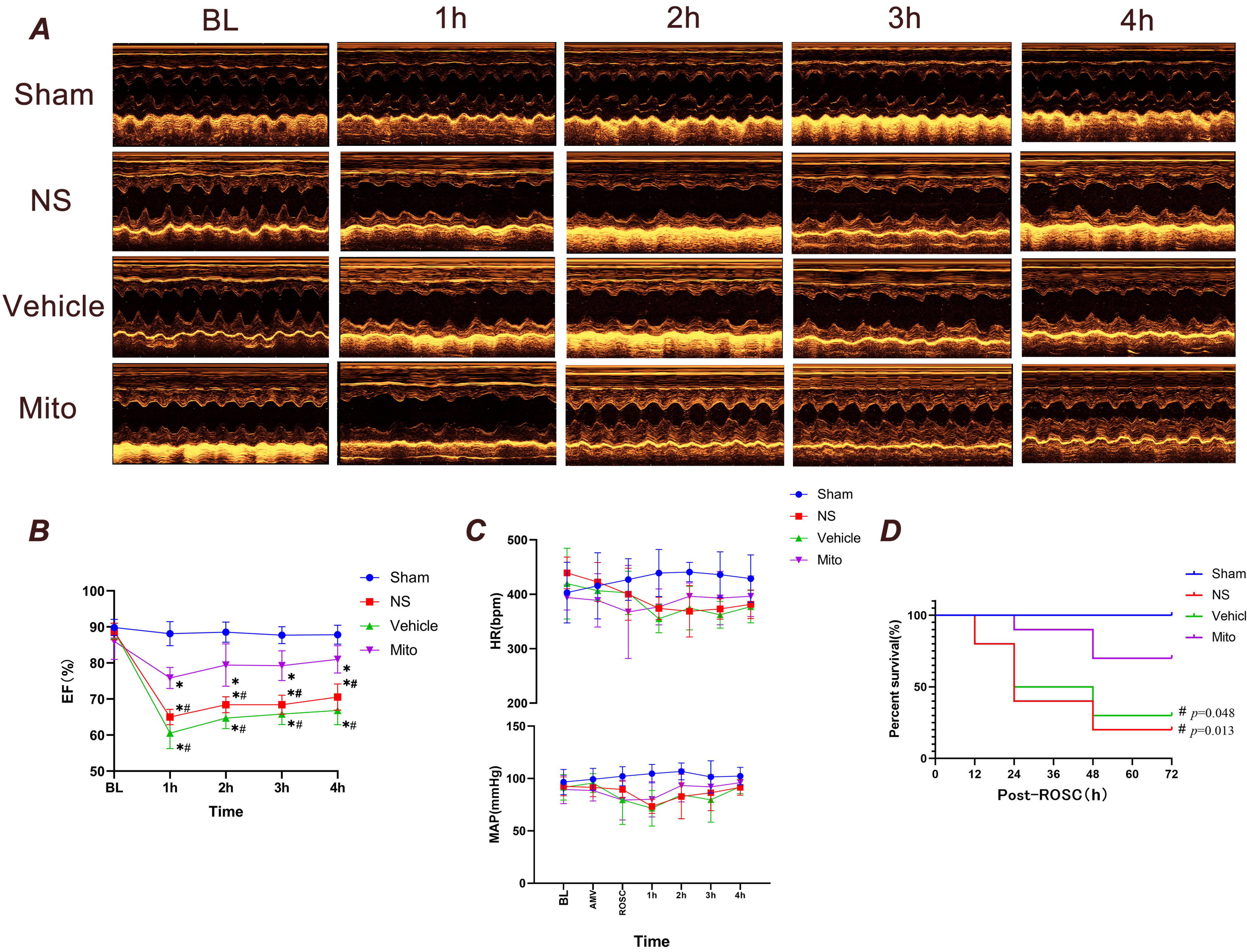
A
BL
1h
2h
3h
4h
Sham
NS
Vehicle
Mito
B
EF(%)
100
90
80
70
60
50
BL
1h
2h
3h
4h
Time
Sham
NS
Vehicle
Mito
*
*#
*#
*
*#
*#
*
*#
*#
*
*#
*#
C
HR(bpm)
500
400
300
200
MAP(mmHg)
150
100
50
0
BL
AMV
ROSC
1h
2h
3h
4h
Time
Sham
NS
Vehicle
Mito
D
Percent survival(%)
100
50
0
0
12
24
36
48
60
72
Post-ROSC(h)
Sham
NS
Vehicle
Mito
# p=0.048
# p=0.013

A
JC-1 aggregates
JC-1 monomers
100 µm
100 µm
B
Mito
Muscle
TOM20
16 kDa
GAPDH
36 kDa
Mito
Muscle
COX IV
17 kDa
GAPDH
36 kDa

DAPI
ACTN2
Mito-tracker
Merge
Sham
NS
Vehicle
Mito
Endocardium
80 μm
20 μm

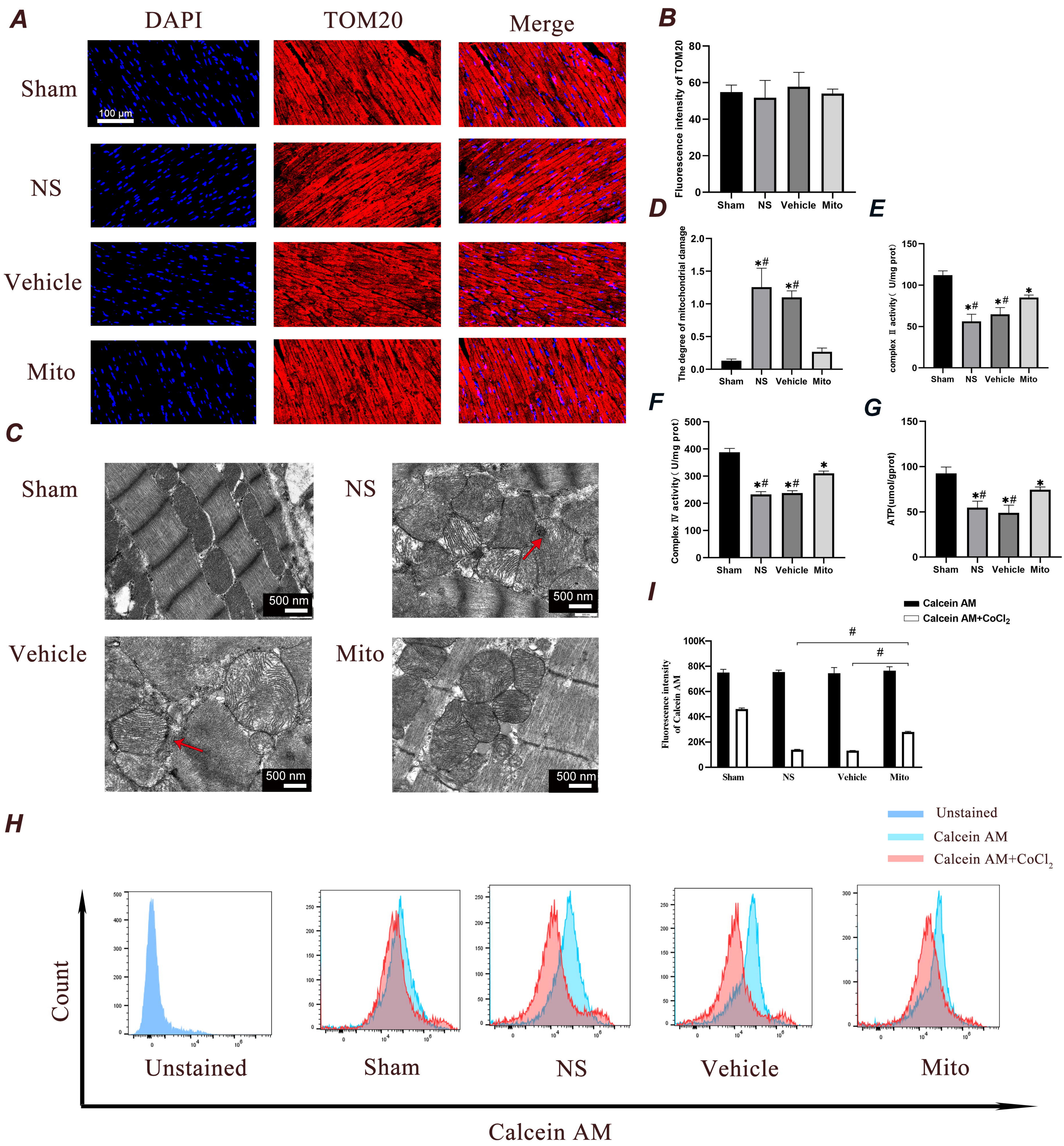
A
DAPI
TOM20
Merge
Sham
NS
Vehicle
Mito
100 μm
B
Fluorescence intensity of TOM20
0
20
40
60
80
Sham
NS
Vehicle
Mito
C
Sham
NS
Vehicle
Mito
500 nm
D
The degree of mitochondrial damage
0.0
0.5
1.0
1.5
2.0
*#
*#
Sham
NS
Vehicle
Mito
E
complex Ⅱ activity（ U/mg prot）
0
50
100
150
*#
*#
*
Sham
NS
Vehicle
Mito
F
Complex Ⅳ activity（ U/mg prot）
0
100
200
300
400
500
*#
*#
*
Sham
NS
Vehicle
Mito
G
ATP(umol/gprot)
0
50
100
150
*#
*#
*
Sham
NS
Vehicle
Mito
I
Calcein AM
Calcein AM+CoCl$_2$
Fluorescence intensity of Calcein AM
0
20K
40K
60K
80K
100K
#
#
Sham
NS
Vehicle
Mito
H
Unstained
Calcein AM
Calcein AM+CoCl$_2$
Count
Unstained
Sham
NS
Vehicle
Mito
Calcein AM

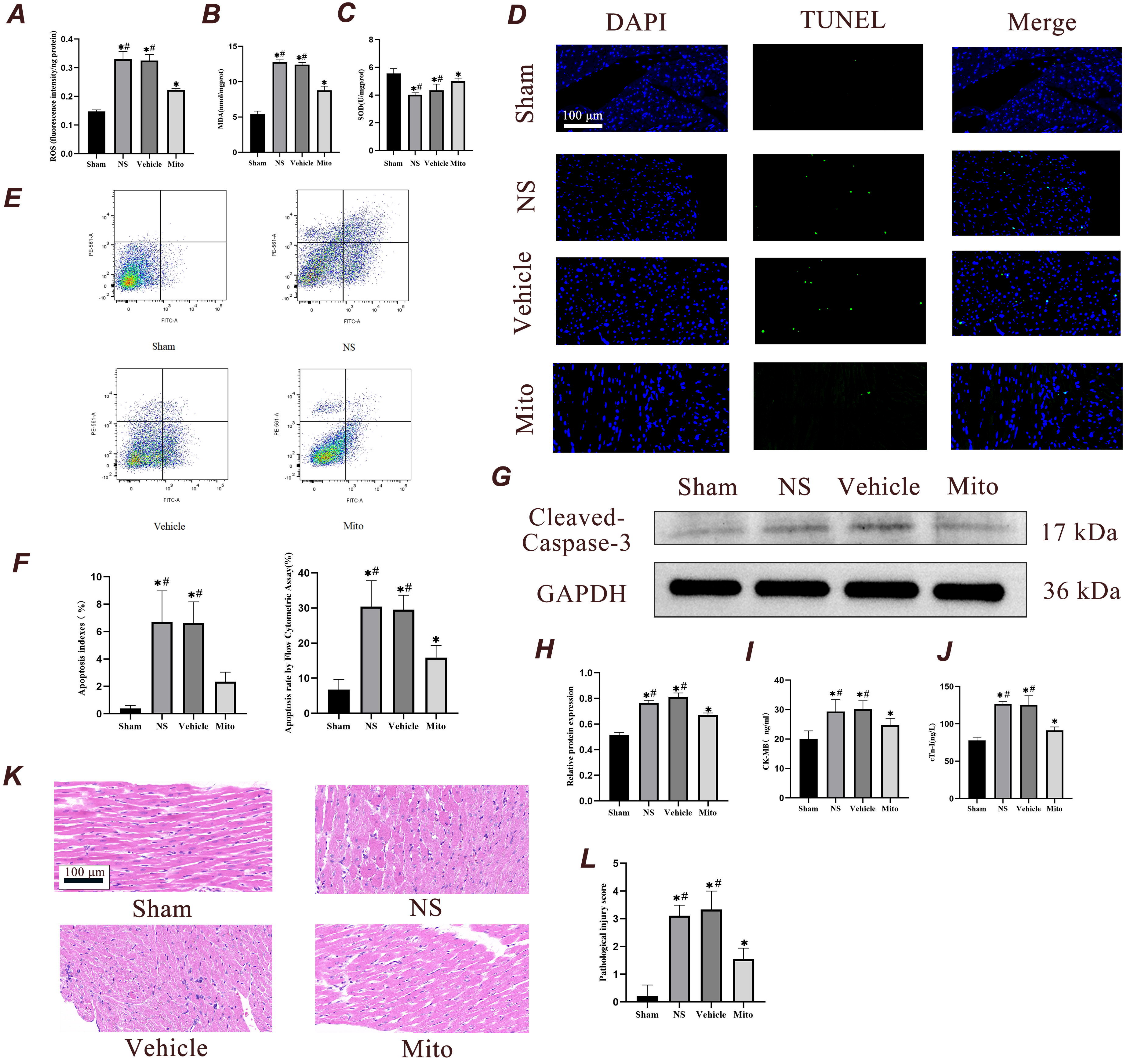
A
ROS (fluorescence intensity/ng protein)
0.0
0.1
0.2
0.3
0.4
Sham
NS
Vehicle
Mito
*#
*#
*
B
MDA(nmol/mgprot)
0
5
10
15
*#
*#
*
C
SOD(U/mgprot)
0
2
4
6
8
*#
*#
*
D
DAPI
TUNEL
Merge
Sham
NS
Vehicle
Mito
100 μm
E
PE-561-A
FITC-A
Sham
NS
Vehicle
Mito
F
Apoptosis indexes（%）
0
2
4
6
8
10
Apoptosis rate by Flow Cytometric Assay(%)
0
10
20
30
40
*#
*#
*
G
Sham
NS
Vehicle
Mito
Cleaved-Caspase-3
GAPDH
17 kDa
36 kDa
H
Relative protein expression
0.0
0.2
0.4
0.6
0.8
1.0
I
CK-MB（ng/ml）
0
10
20
30
40
J
cTn-I(ng/L)
0
50
100
150
K
100 μm
Sham
NS
Vehicle
Mito
L
Pathological injury score
0
1
2
3
4
5

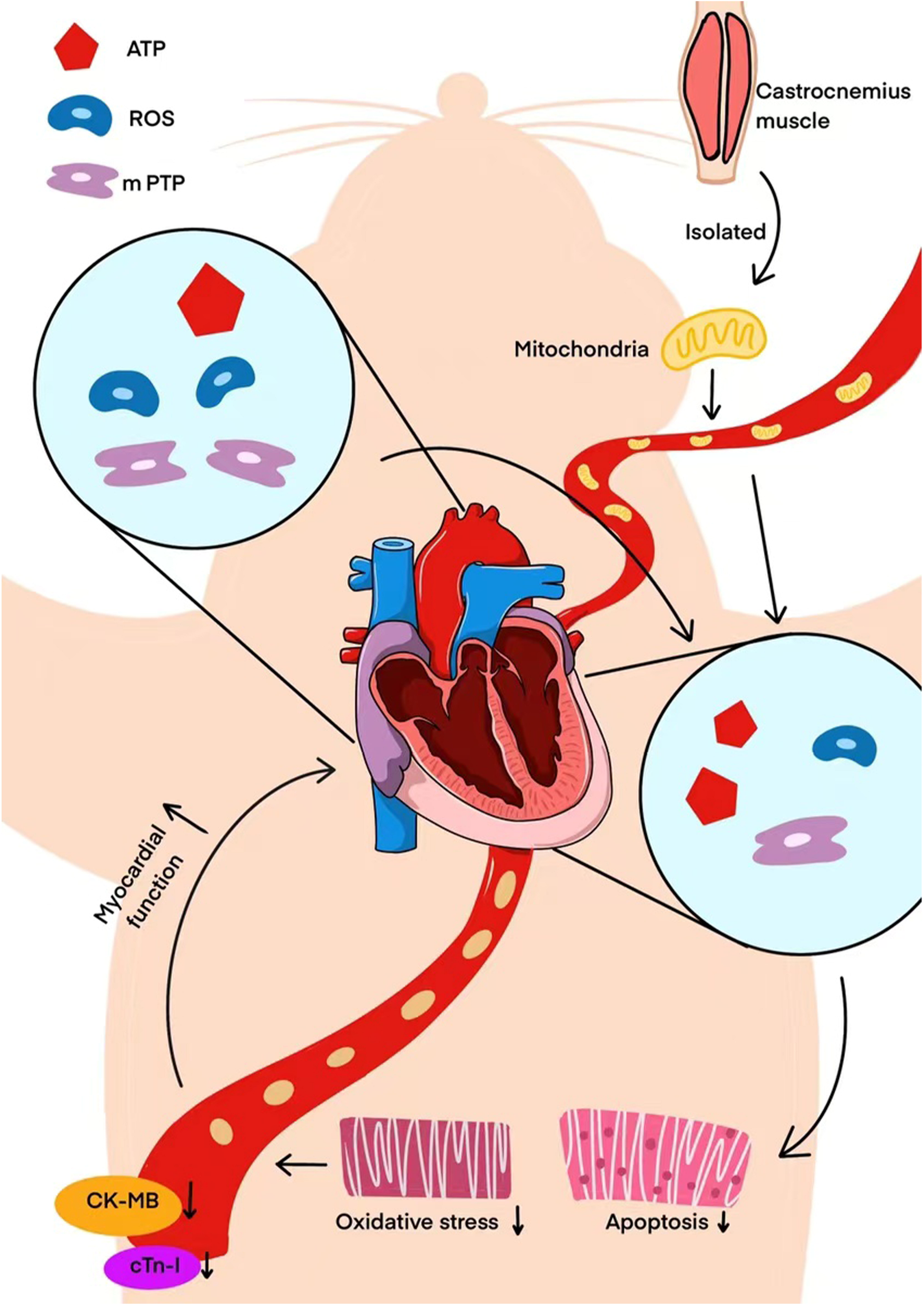
ATP
ROS
m PTP
Castrocnemius muscle
Isolated
Mitochondria
Myocardial function ↑
CK-MB ↓
cTn-I ↓
Oxidative stress ↓
Apoptosis ↓